

Effect of alloying element addition on the microstructural evolution and corrosion behaviour of Fe-30 at. % (Al + Cr) alloys.

Z. Belamri^{a*}, D. Hamana^{a,b}, A. Azizi^a, L. Boumaza^a and A. Haddad^a

^aUnité de Recherche Sciences des Matériaux et Applications, Université Frères Mentouri Constantine 1, Route Ain El-Bey, Constantine 25000, Algérie.

^bEcole Nationale polytechnique de Constantine, PB 75 RP Ali Mendjeli, Constantine 2500, Algérie.

*Corresponding author, email: zahirabelamri@hotmail.com

Selected paper of JSSE'18, received in final form: March 5, 2019 ; accepted date: March 23, 2019

Abstract

Fe-Al and Fe-Al-Cr alloys have interest industrial and biomedical applications for their excellent properties. Two materials of nominal composition Fe-30 at. % Al and Fe-15 at. % Al-15 at. % Cr have been examined. The aim of this present work is: first, study the order-disorder transformations in these alloys. Second, the effect of partial substitution of Al by Cr in Fe matrix on the microstructural evolution and corrosion behaviour of two iron-based alloys. DSC analyses, XRD, microhardness measurements, SEM analyses and electrochemical measurements have been carried out. The obtained results show that during heating the studied alloys undergo order-disorder and disorder-order transformations. The presence of Cr influences the ordering process of the $D0_3$ ordered phase and also varies the microhardness of these materials. During corrosion test in salt water, the chromium oxide layer (Cr_2O_3) forms on the surface of Fe-15 at. % Al-15 at. % Cr alloy and also increases its corrosion resistance. It is necessary to remember that the formation of $D0_3$ ordered phase has an effect on the electrochemical parameters. These results are a good agreement with the published works.

Keywords: order-disorder transition; $D0_3$ ordered phase; iron-based alloys; corrosion

1. Introduction

Fe-Al alloys, especially at the iron-rich Fe-Al system, belong to the most widely studied intermetallics for structural and functional applications [1]. Fe_3Al refers to the Fe-Al intermetallic compound with Al atom fraction between 23% and 32%. Fe_3Al is cheap and can be smelted and processed with iron and aluminum. The resistance to the oxidation, sulfuration, nitric acid corrosion and wear properties of Fe_3Al are excellent and its high temperature strength and high temperature creep resistance are better than most of metal [2].

These materials are also considered for room temperature application in place of stainless steels, for example, pipes and tubes for heating elements, and in distillation and desalination plants [3]. The field of application of the ternary Fe-Al-Cr alloys is quite wide, essentially as substrates for catalysts applied in catalytic converters and filter systems in automobiles [4].

In addition to this, these materials are also considered for biomedical applications, such as bone joints and surgical instruments [3]. For testing durability of Fe-Al alloys during working conditions in a corrosive environment, corrosion study of these alloys is necessary. The formation of aluminum oxide is thermodynamically more favorable than iron oxide since oxygen has a higher affinity to Al compared to Fe (the standard Gibbs energy of formation of α -

Al_2O_3 is 1,582,260 J/mol which is almost 6.5 times higher compared to FeO) [5, 6].

The aim of this work is to study the effect of alloying element addition, and the order-disorder transformation on the microstructural evolution and corrosion behaviour of Fe-30 at. % (Al+Cr) alloys. Mechanical properties are studied as well by measuring microhardness as function of the ordered state.

2. Experimental methods

The iron-based alloys selected in this study are the following nominal composition of Fe-30 at. % Al and Fe-15 at. % Al-15 at. % Cr. The phase transformations in these alloys have been studied by DSC analyses with a heating rate of 10°C/min. it's carried out under argon using a SETARAM 131 DSC. A ZWICK apparatus connected to a computer with suitable software giving automatic measurements was used for the microhardness measurements ($HV_{0.05}$) using 300 gf load.

A Jeol FEG JSM-7100F scanning electron microscope (SEM) was also used for microstructural observation. The assembly used for the electrochemical measurements involves a Bio-Logic SAS SP-300 type potentiostat. Suitable software used for acquisition and procession of digital data.

3. Results

3.1. DSC analysis

DSC analyses have given a general idea on studied alloys behaviour during a heating and they have been interpreted on the light of the literature and the Fe-Al phase diagram [7]. DSC curve of Fe-30 at. % Al alloy homogenised 2 h at 1100°C and water quenched (fig. 1a) shows the following effects:

- An exothermic peak with a maximum situated at 270°C linked to the $D0_3$ ordered phase formation,
- A splitted endothermic peak in the temperature range [440-530°C], the first peak with a minimum at 470°C linked to the gradual decrease of $D0_3$ ordered phase and a second peak between 480 and 530°C with a minimum around 511°C, related to the formation of B2 semi-ordered phase.

The $D0_3$ ordered phase has also appeared in the Fe-15 at. % Al-15 at. % Cr alloy homogenised 2 h at 1100°C and water quenched, where its DSC curve (fig. 1b) shows the following effects:

- The formation of the $D0_3$ ordered phase in this alloy is around 284°C. Golovin [8] proved that in the Fe-15% at. Al-15% at. Cr alloy long range order is not detected by the TEM but superdislocations that are typical of the order of the $D0_3$ structure can be detected, while only XRD analysis indicates a certain order as observed in this study (fig. 3b). No transitions are referred to precipitate are observed. According to Palm [9] it is found in Fe-Al-Cr system that only at higher Al contents (higher than 50% Al) the possibility of precipitating of second phase, e.g. hexagonal Al_3Cr , exists.
- An endothermic peak around 538°C due to order-disorder transition.

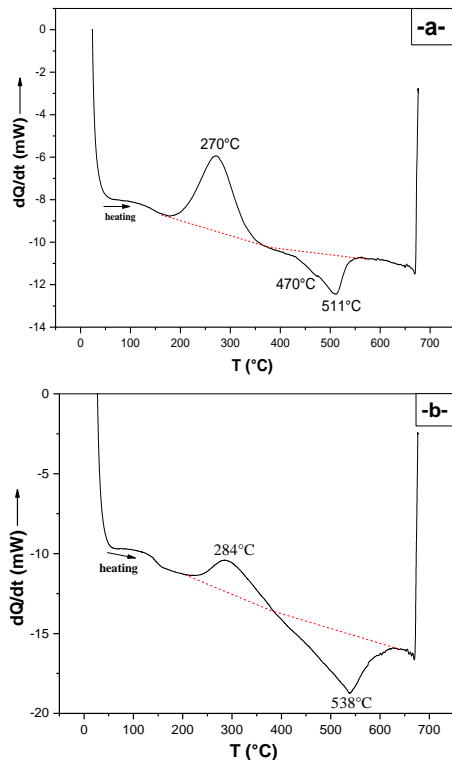


Figure 1. DSC curves obtained with heating rate of 10°C/min of homogenised 2 h at 1100°C and water quenched alloys: (a) Fe-30 at. % Al and (b) Fe-15 at. % Al-15 at. % Cr.

3.2. Microhardness measurements

As it has been shown in several studies, the mechanical properties of Fe-Al alloys can be modified by Cr addition in Fe-Al alloys. In this part we studied the microhardness variations as function of the annealing time at the temperature of the $D0_3$ ordered phase formation. Microhardness measurements show that the formation of the $D0_3$ ordered phase leads to increase of microhardness values for the two studied alloys. For the Fe-30 at. % Al alloy (fig. 2a), it reaches its maximum value (316.8 N/mm²) after annealing for 3 h at 270°C. This increase is due to the formation of the $D0_3$ ordered phase and the increase of their antiphase domains fraction which leads to the difficulty of dislocation deviation. Annealing of the same alloy at the same temperature up to 6 hours leads to a decrease in microhardness up to 298 N/mm². This decrease is justified by the coalescence of antiphase domains (PAPhs). The formation of this phase is confirmed by XRD (fig. 3a).

For the Fe-15 at. % Al-15 at. % Cr alloy (fig. 2b), the microhardness increases to reach its maximum value (243.5 N/mm²) after annealing 60 min at 284°C. This increase is also justified by the formation of the $D0_3$ ordered phase and increasing of its antiphase domains fraction to the complete transformation of α disordered phase to the $D0_3$ ordered phase. Figure 3b shows that annealing for 1 h at 284°C of Fe-15 at. % Al-15 at. % Cr leads to the formation of $D0_3$ ordered phase. Increasing of annealing time to 2,5 hours at the same temperature leads to the decrease in microhardness up to 216.7 N/mm² which explained by the coalescence of antiphase domains (PAPh). It's noted that the maximum value of microhardness is reached more rapidly in the alloy with Cr addition than the one without Cr. This shift can be explained by the effect of the Cr addition which accelerates the coalescence process of antiphases domains. Substitution of Al atoms by Cr in Fe-30 at. % (Al + Cr) studied alloys leads to the decrease of microhardness, whether at quenching state or in the annealed state at the temperature of formation of the $D0_3$ ordered phase.

3.3. Electrochemical measurements

The electrochemical parameters of the studied alloys are derived from polarization curves and summarized in table 1. The values of the potential (E_{corr}), the corrosion current (I_{corr}) and corrosion rate (V_{corr}) are obtained by drawing of the Tafel's line using a software of electrochemical apparatus. Polarization resistance (R_p) is calculated using the following equation Hissel [10-12]:

$$R_p = \left(\frac{\Delta E}{\Delta I} \right) = \left(\frac{1}{2.303 I_{corr}} \right) \left(\frac{\beta_a \cdot \beta_b}{\beta_a + \beta_b} \right) = \frac{B}{I_{corr}} \quad (1)$$

I_{corr} : Current intensity of corrosion measured experimentally (mA/cm^2).
 β_a and β_b are the slopes of Tafel's line

the surface is covered by a very thick oxide film layer (corrosion products).

Table 1: Electrochemical parameters of the treated Fe-30 at. % Al and Fe-15 at. % Al-15 at. % Cr alloys.

Alloys	$-E_{corr}$ (mV)	I_{corr} ($\mu\text{A}/\text{cm}^2$)	β_c (mv)	β_a (mv)	V_c	R_p ($\Omega.\text{cm}^2$)
Fe-30 at. % Al homogenised and water quenched	752.478	36.34	263	321.1	$10.732 \cdot 10^{-3}$	$2.3834 \cdot 10^3$
Fe-15 at.% Al-15 at.% Cr homogenised and water quenched	759.494	23.286	253.8	312.1	$4.0179 \cdot 10^{-3}$	$2.6097 \cdot 10^3$
Fe- 30 at % Al homogenised and air cooling.	601.288	3.585	245.9	280.2	$1.2169 \cdot 10^{-3}$	$6.2682 \cdot 10^3$
Fe-15 at.% Al-15 at.% Cr homogenised and air cooling.	659.858	4.934	231.1	311.9	$1.9344 \cdot 10^{-4}$	$1.1682 \cdot 10^4$

Zamanzade et al. [5] were found that the shape and the characteristics of polarization curves are very sensitive to a certain number of factors such as the composition of the alloy, their thermal history, their structural state, etc.....So the effect of the ordered state and the alloys composition must be studied in this work.

3.3.1. Effect of the $D0_3$ ordered phase formation

Figures 4 (a-b) show that the corrosion potential is shifted to more negative values in salt water for the two studied alloys at the disordered state (quenched from 1100°C), compared to the ordered state (air cooled from 1100°C). This shift is accompanied by increasing of the current density (table 1), so we can say that the erosion of this alloys in the disordered state is faster than the alloy in the ordered state.

Since the polarization resistance (R_p) represents the capacity of the material to prevent current flow in a given medium, and then R_p is inversely proportional to I_{corr} , then the increase in the density of I_{corr} is associated by a decrease in the value of polarization resistance, and the presence of Cl⁻ ions increases the current flow in the medium by reducing the ability of the metal to prevent this flow.

3.3.2. Effect of Cr addition

Polarization curves shown in the figures 4 (c-d) indicate that Fe-15 at. % Al-15 at. % Cr alloy is more resistant to corrosion in salt water; this is caused by the presence of chromium. The chromium oxide layer (Cr_2O_3) that forms on the surface of Fe-15 at. % Al-15 at. % Cr alloy homogenized 2h at 1100°C and air-cooled do not dissolve easily by reaction with OH⁻ ions.

The SEM images of Fe-30 at. % Al and Fe-15 at. % Al- 15 at. % Cr alloys in figures 5 and 6 show that

The percentages for the elements found by EDS analysis were presented also. The decrease in Fe content in the two studied alloys after corrosion proves that they are covered with the oxide film. Decrease of Al and Cr content in alloys after immersion in aqueous solution of 0.1 M NaCl could be attributed to the dissolution of Al and Cr due to the chloride ions attack.

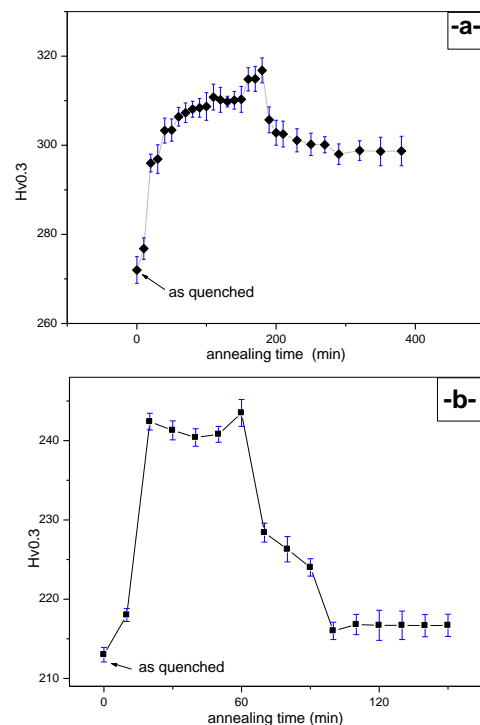


Figure 2. Variation of the microhardness as function of annealing time after homogenised and water quenched alloys: (a) Fe-30 at. % Al alloy annealing at 270°C , (b) Fe-15 at. % Al -15 at. % Cr alloy annealing at 284°C .

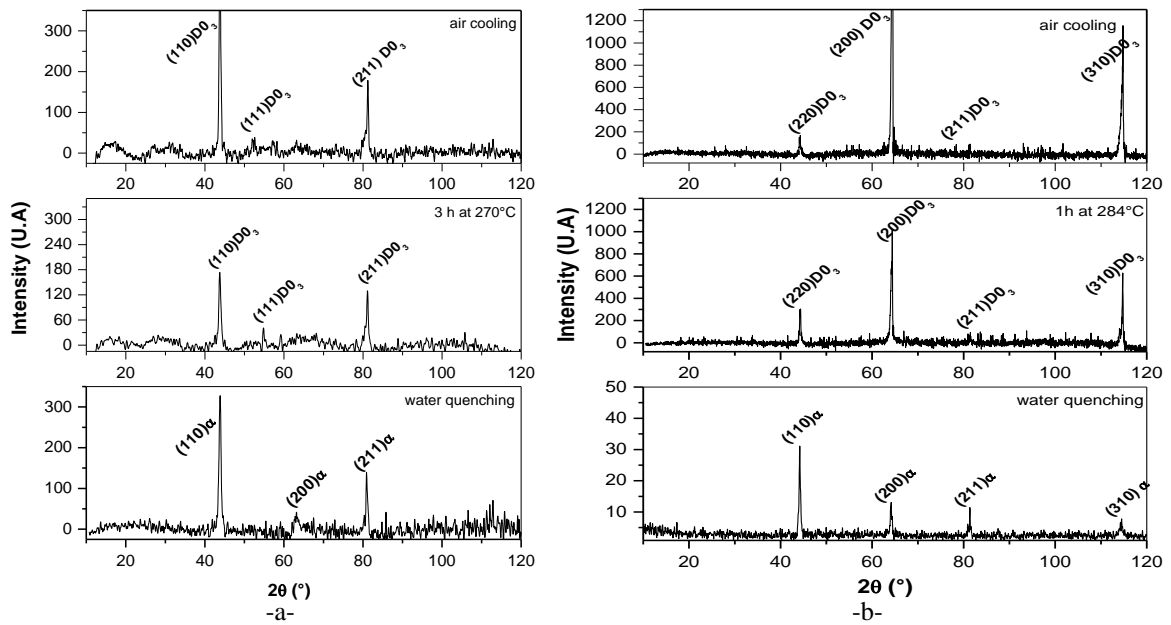


Figure 3. XRD patterns of studied alloys after homogenised and water quenched then annealing: (a) Fe-30 at. % Al and (b) Fe-15 at. % Al- 15 at. % Cr

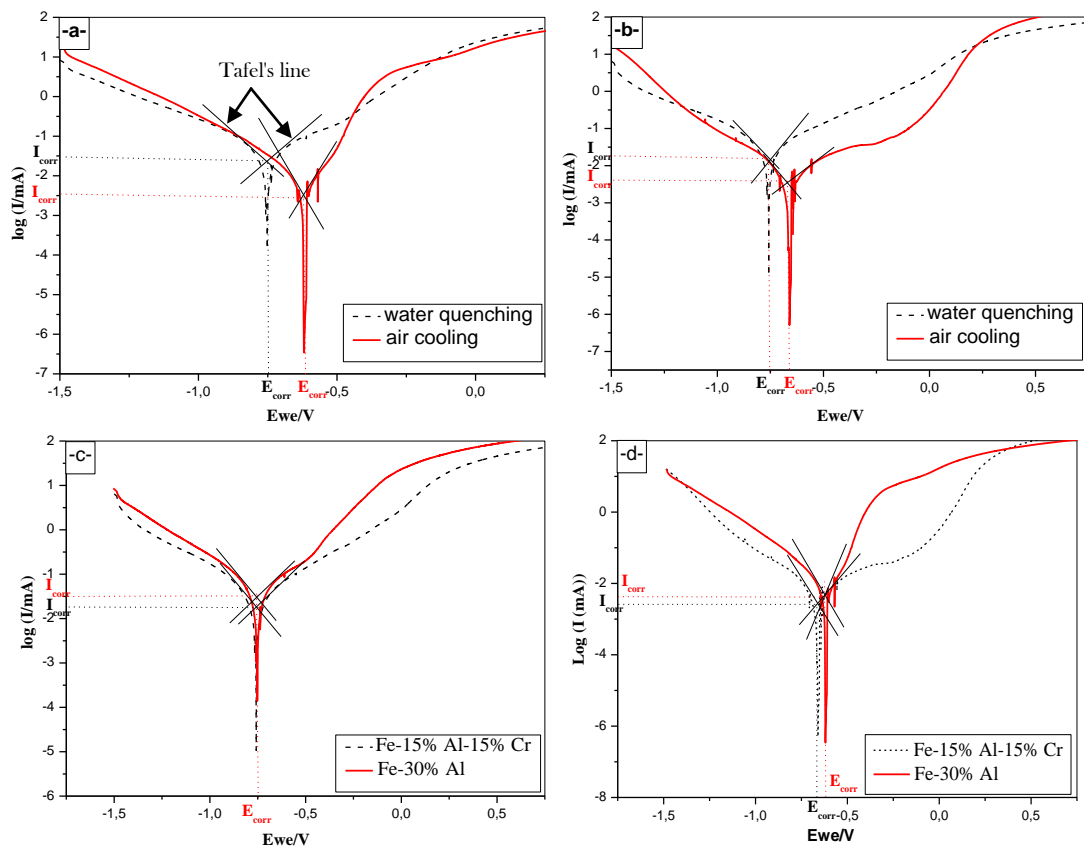


Figure 4. Polarisation curves of studied alloys immersed in 0, 1 M NaCl :

- Fe-30 at. % Al alloy homogenised for 2 h at 1100°C then : water quenching or air cooling,
- Fe-15 at. % Al-15 at.% Cr alloy homogenised for 2 h at 1100°C then : water quenched or air cooling,
- Fe-15 at. % Al-15 at. % Cr and Fe-30 at. % Al alloys homogenised for 2 h at 1100°C then water quenched,
- Fe-15 at. % Al-15 at. % Cr and Fe-30 at. % Al alloys homogenised for 2 h at 1100°C then air cooling.

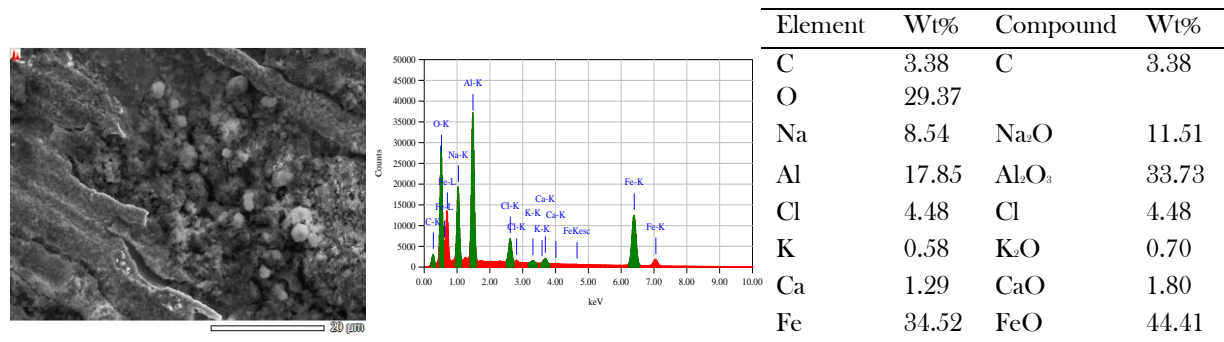


Figure 5. Spectrum EDS and the table inserted show the concentration of the various components of the Fe-30 at. % Al alloy homogenised then air cooling after corrosion test.

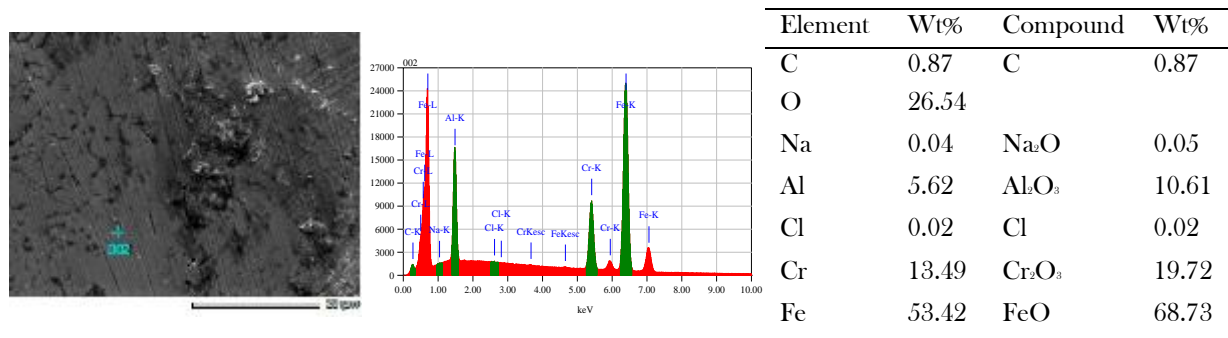


Figure 6. Spectrum EDS and the table inserted show the concentration of the various components of the Fe-15 at. % Al-15 at. % Cr alloy homogenised then air cooling after corrosion test.

4. Conclusion

The present work is a study of the effect of Cr substitution on the physical properties of these alloys. Two types of iron-based alloys are studied: Fe-30 at. % Al and Fe-15 at. % Al-15 at. % Cr. DSC analyses show different phase transitions during heating of studied alloys. This is confirmed by XRD analysis where superstructure peaks are observed on XRD spectrum of air cooling and annealing samples. The formation of the D0₃ ordered phase leads to the increase of microhardness for the two studied alloys. The maximum value of the microhardness is reached more rapidly in the alloy with Cr addition. The substitution of Al atoms by Cr in Fe-30 at. % (Al + Cr) alloys leads to the decrease of microhardness. Presence of chromium confers to Fe-15 at. % Al-15 at. % Cr alloy a good resistant to corrosion in salt water in comparison to alloy without chromium. The formation of the ordered phase slows the electrochemical processes in the studied alloy.

References

- [1] F. Stein, A. Schneider, G. Frommeyer, *Intermetallics*, 11 (2003) 71.
- [2] B. Wang, C. Cui, S. Zhang, J. Bai, *Materials Chemistry and Physics*, 198 (2017) 7.
- [3] F. Rosalbino, R. Carlini, R. Parodi, G. Zanicchi, *electrochimica Acta*, 62 (2012) 305.
- [4] H. Michel, G. Jacobs, S. F. Rainer, *CALPHAD: Computer Coupling of Phase Diagrams and Thermochemistry* 33 (2009) 170.
- [5] M. Zamanzade, A. Barnoush, C. Motz, *Crystals*, 10 (2016) 1.
- [6] M. Zamanzade, A. Barnoush, *Corrosion Science*, 78 (2014) 223.
- [7] S. C. Vogel, F. Stein, M. Palm, *Appl Phys A*, (2010) 607.
- [8] I. S. Golovin, *Materials Science and Engineering*, 442 (2006) 92.
- [9] M. Palm, *Intermetallics*, 13 (2005) 1286.
- [10] J. Hissel, *Corrosion Science*, 14 (1974) 293.
- [11] M. Stern, A.L. Geary, *J. Electrochem. Soc.*, 104 (1957) 56.
- [12] Document: Corrosion Part 3-Measurement of Polarization Resistance, AN-COR-003, (2018). https://partners.metrohm.com/GetDocument?action=get_dms_document&docid=2044490